Amputation induces stem cell mobilization to sites of injury during planarian regeneration

Otto C. Guedelhoefer, IV[1] and Alejandro Sánchez Alvarado[1,2,]*

SUMMARY

How adult stem cell populations are recruited for tissue renewal and repair is a fundamental question of biology. Mobilization of stem cells out of their niches followed by correct migration and differentiation at a site of tissue turnover or injury are important requirements for proper tissue maintenance and regeneration. However, we understand little about the mechanisms that control this process, possibly because the best studied vertebrate adult stem cell systems are not readily amenable to in vivo observation. Furthermore, few clear examples of the recruitment of fully potent stem cells, compared with limited progenitors, are known. Here, we show that planarian stem cells directionally migrate to amputation sites during regeneration. We also show that during tissue homeostasis they are stationary. Our study not only uncovers the existence of specific recruitment mechanisms elicited by amputation, but also sets the stage for the systematic characterization of evolutionarily conserved stem cell regulatory processes likely to inform stem cell function and dysfunction in higher organisms, including humans.

KEY WORDS: Stem cells, Regeneration, Tissue repair, Tissue homeostasis, Stem cell migration, Stem cells recruitment, Planaria

INTRODUCTION

During development, morphogenesis occurs in a predictable pattern that deviates little between individuals within a species. Thus, embryonic cell migration and proliferation have evolved such that tissue progenitor cells arrive at correct locations and with sufficient numbers as tissues form de novo. During regeneration after injury, however, which tissues will require repair and rebuilding cannot be predicted. Although recruitment of progenitor cells to the wound site seems therefore likely, such mechanisms are poorly understood (Daley and Scadden, 2008).

In terms of human health, understanding the signals that stem and progenitor cells use to navigate within an organism is of the utmost importance as we develop stem cell (SC) therapies (Karp and Leng Teo, 2009). Such therapies have existed for nearly half a century (Congdon, 1971), and a recent surge in potential therapies has accompanied the discovery of new mammalian adult SC populations (Pittenger et al., 1999; Rietze et al., 2001; Blanpain et al., 2004; Sherwood et al., 2004). These therapies have quickly advanced to clinical trials regardless of our poor understanding of the factors that control SC movement. A better understanding of adult SC migration would not only serve to improve the efficacy of therapies, but might also provide novel approaches to combat cancer metastasis given the stem-cell-like nature of cancer progenitors (Reya et al., 2001).

Mammalian factors involved in homeostatic migration of hematopoietic stem cells (HSC) and wound response migration of muscle satellite cells have been identified (Laird et al., 2008). However, in vivo observation of adult SC migration in these systems requires highly technical imaging that is hampered by low resolution (Kim et al., 2007). Study of adult SC migration in vertebrates is further complicated by their multifarious anatomy and varied regenerative potential. There is a clear need for a simpler animal model of adult SC migration that possesses efficient regeneration and can be easily manipulated.

The planarian *Schmidtea mediterranea* is uniquely suited to investigations of adult SC migration owing to its remarkable regeneration and simple body plan (Newmark and Sánchez Alvarado, 2002). Regeneration of any missing or damaged body part is made possible by a population of adult SCs called neoblasts (Wolff and Dubois, 1948; Dubois, 1949; Fedecka-Bruner, 1965). Within this population are clonogenic SCs that are singly capable of reconstituting an entire animal (Wagner et al., 2011). Exposure to ionizing radiation abolishes regeneration in planarians by specifically ablating SCs (Hayashi et al., 2006).

For over a century, researchers have hypothesized that these cells migrate from distant sites to a wound during regeneration (Lehnert, 1891). The evidence for SC migration in planaria has been contradictory. Partial irradiation experiments using lead to shield a population of SCs in an irradiated animal indirectly demonstrated that SCs might migrate through irradiated tissue to reach a distant wound (Dubois, 1949). More recent studies, however, have produced conflicting results, largely because they lacked reliable SC markers (Stéphan-Dubois and Lender, 1956; Saló and Baguñà, 1985). These findings have not been revisited.

Here, we show that planarian SCs, although stationary during tissue homeostasis, are mobilized following wounding. We demonstrate that both resident and introduced SCs were capable of directional responses to amputation. We illustrate how SC migration repopulates the SC compartment and re-establishes progeny production, restoring long-term tissue homeostasis and regeneration in lethally irradiated animals. This study demonstrates that planarian tissue transplantation and partial irradiation are powerful and efficient techniques for evaluating the movements of SCs and their progeny, establishing planaria as an effective model for studying the mechanisms underlying SC recruitment.

[1]Department of Neurobiology and Anatomy, University of Utah School of Medicine, Salt Lake City, UT 84132, USA. [2]Howard Hughes Medical Institute, Stowers Institute for Medical Research, 1000 E 50th St Kansas City, MO 64110, USA.

*Author for correspondence (asa@stowers.org)

MATERIALS AND METHODS

Planaria
Asexual *Schmidtea mediterranea* (Sánchez Alvarado et al., 2002) were maintained (Cebrià and Newmark, 2005) and fed two to three times per week. Hermaphroditic (sexual) animals of the CIWsx2 clonal line were maintained (Newmark and Sánchez Alvarado, 2000) and fed once per week. All animals used were >1 cm in length and were starved for 1 week prior to manipulation.

Immobilization
For partial irradiation and transplantation, animals were anesthetized by immersion in ice-chilled 0.1-0.2% chloretone for 5-10 minutes.

X-ray partial irradiation
Immobilized animals were arranged on wet filter paper in a Petri dish on ice. Custom-manufactured lead shields (supplementary material Fig. S1) were centered along each animal's longitudinal axis. Animals were positioned 30 cm from the x-ray and a dose of ~30 Gy (3.6 minutes at 320 kV 10 mA, no hardening filter) was delivered.

RNA whole-mount in situ hybridization (WISH)
WISH was performed as described (Pearson et al., 2009) with the following alterations for use with large animals: no nutation; 10% N-acetylcysteine; 30 minutes fixation; additional 10 minutes 1% SDS (in PBS) treatment after fixation; 20 minutes Proteinase K treatment at 37°C; hybridization solution contained 50% formamide, 5× SSC, 1× Denhardts, 1 mg/ml yeast RNA, 100 µg/ml heparin, 0.05% Triton-TX, 0.05% Tween-20, 50 mM DTT, 5% dextran sulfate and 1% SDS; digoxigenin-labeled riboprobes were used for all single-color WISH and dinitrophenol-labeled riboprobes were added for double-color WISH; 50% PVA was added to NBT/BCIP development buffer. Development with DAB was performed in 5% PVA with 2× ImmPACT DAB chromogen (Vector Labs), 0.01% H_2O_2 in ImmPACT DAB diluent for 30 minutes. Only NBT/BCIP developed specimens were mounted in 80% glycerol and all others were in Murray's Clear.

γ-Irradiation
γ-Irradiation (100 Gy) was performed as previously described (Eisenhoffer et al., 2008).

Tissue transplantation
Microsurgery protocols were based on previous work (Santos, 1929; Kato et al., 1999). Capillary tubes of 0.75 mm interior diameter and 0.7 mm exterior diameter (FHC, Bowdoin, ME, USA) were used to excise graft tissue and remove host tissue from the future transplantation site, respectively. Using forceps graft tissues were inserted into the host and then completed transplantations were transferred on filter paper into recovery chambers (supplementary material Fig. S2). Operated animals were allowed to recover at 10°C overnight.

Karyotyping
Animals were karyotyped at long-term follow-up (>1 year post transplantation) by placing animals in 0.05% colchicine overnight and fixing for 15 minutes in 3:1 ethanol and acetic acid. Animals were then treated for 2 minutes in 1N HCl at room temperature (RT) then for 6 minutes at 60°C. HCl was replaced with acetic orcein for 15 minutes. Animals were then treated for 5 minutes each in 60% acetic acid then 1:1:1 lactic acid, acetic acid, and water. Specimens were placed on a Superfrost Plus glass slide (VWR), squashed with a siliconized coverslip (Hampton Research), and allowed to settle overnight. Slides were frozen in liquid N_2, coverslips removed with a razorblade, and submerged in cold ethanol mixed with dry ice. Slides were warmed to RT, air dried, stained with 0.5 µg/ml propidium iodide for 30 minutes, rinsed with water, and mounted in Vectashield.

Immunostaining
Animals were killed, fixed, reduced and permeabilized as described for WISH. WISH was performed first when immunostaining was performed in combination. When performed alone, animals were treated for 30 minutes in 3% formamide, 6% H_2O_2 in PBST (0.05% Triton-TX) and

bleached overnight in 6% H_2O_2 in PBST. Animals were blocked in 1% BSA (Sigma) with 1% horse serum (Sigma) or 1% goat serum (Sigma) for 4 hours. Incubation with anti-phosphohistone H3 (anti-H3P, Millipore) at 1:300 was performed overnight at room temperature. Anti-H3P was detected with either 1:100 anti-rabbit-HRP (Zymax) and subsequent tyramide amplification as described (Reddien et al., 2005a), or with 1:300 anti-rabbit-Alexa555 (Invitrogen). Specimens were mounted in either 80% glycerol or Murray's Clear.

Image acquisition and manipulation
Live animal and NBT/BCIP developed images were captured on a Zeiss Lumar v.12 with an Axiocam HRc; except for NBT/BCIP and DAB double images, which were captured on Zeiss AxioVert with extended focal distance rendering by CombineZP. Color and gamma adjustments were made using Zeiss AxioVision v.3-4.1. Levels were adjusted and backgrounds cropped in Adobe Photoshop.

Fluorescent images were captured on a Zeiss LSM 5 LIVE confocal microscope using RealTime automation for image concatenation. Lack of autofluorescence when excited with 488 nm λ laser was used to identify the graft-host boundary in transplantations (Figs 3-5). All images are z-projections except where noted (Fig. 4S-V). Scaled LSM files were level adjusted, channel mixed, and cropped using NIH ImageJ.

Image analysis and quantification
Image quantification was performed using NIH ImageJ. The length of the cell bands in partially irradiated animals was measured along the midline from the most anterior cell to the most posterior cell on both ventral and dorsal sides (Fig. 1K).

The distance of H3P(+) foci from the graft boundary (Fig. 3K, Fig. 5M) was determined using the Cell Counter function of ImageJ. Measurements were combined into 45° bins centered on the pictured axes (Fig. 4K). Cells inside the graft were not analyzed. Raw data were imported into R (http://www.r-project.org/).

Rendering for the mean distance from the center of the graft measurements in WISH specimens (Fig. 5J) was carried out using the Polar Transformer function of ImageJ. The Cell Counter function was used to measure distances of all cells that could be individually resolved. The data was combined into 45° bins centered on the anterior, posterior, right and left axes.

Dispersion in partially irradiated animals was calculated as the mean standard error in the relative longitudinal location of the 50 most anterior or posterior cells. The image analysis procedure was equivalent for anterior and posterior boundaries. The relative y positions of cells in oriented and scaled images were determined using the Cell Counter function and mean s.e.m. values were computed (Fig. 6G).

RESULTS

Stem cells migrate minimally in the absence of a wound
To study adult SC migration, we first established the baseline level of SC migration in intact planarians. X-ray irradiated planarians are known to degenerate and eventually disintegrate (Bardeen and Baetjer, 1904) and SC ablation by ionizing radiation is well established in planaria (Reddien et al., 2005b). We therefore developed a method of irradiating anterior and posterior portions of planaria while protecting consistently sized mid-sections using identical lead shields (Fig. 1A).

Using this new method, we investigated whether SCs from the shielded portion migrate in the absence of wounding. We partially irradiated a cohort of animals and analyzed their gross morphology over time (Fig. 1B-E). The animals initially looked normal (Fig. 1B), but soon displayed head regression (Fig. 1C,C′) and complete head resorption (Fig. 1D,D′). Complete regression of irradiated tissues in partially irradiated animals has been described previously (Dubois, 1949); however, we observed only partial regression of the irradiated tissues. Animals were observed to regenerate their
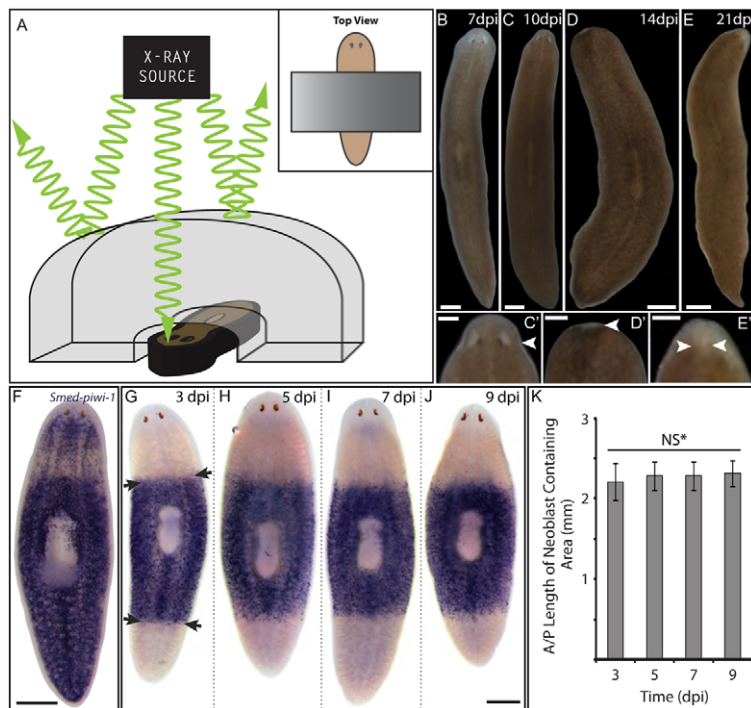
Fig. 1. SCs do not migrate in intact partially irradiated planaria. (**A**) Partial x-ray irradiation with lead shield (gray). Anterior and posterior ends (inset) receive lethal doses (~30 Gy) and mid-section receives minimal dose. (**B-E'**) Live images of partially irradiated worms at 7, 10, 14 and 21 dpi. Planaria appeared normal at 7 dpi (B), showed head regression (C', arrowhead) at 10 dpi (C), head resorption (D', arrowhead) at 14 dpi (D), and regenerated heads (E) with photoreceptors (E', arrowheads) at 21 dpi. (**F**) WISH for *Smed-piwi-1* in non-irradiated planaria labels all SCs. (**G-J**) WISH for *piwi* in partially irradiated animals at 3 dpi shows that SCs are absent from unshielded regions and boundaries (arrows) are clear (G). Time course (3, 5, 7 and 9 dpi) shows that the pattern seen at 3 dpi remains largely unchanged (animals to scale). By 9 dpi (J), slight head regression prompted the end of the time course. (**K**) No significant difference (NS*, $P>0.1$, one-way ANOVA) in the length of the cell band was seen between 3 ($n=9$), 5 ($n=9$), 7 ($n=8$) and 9 ($n=7$) dpi. Scale bars: in A-K, 500 μm; in C',D',E', 200 μm.

heads at various times following irradiation but before full regression of the irradiated tissue (Fig. 1E,E'). Subsequently, partially irradiated animals survived ($n=8$) an irradiation dose that was lethal to unshielded animals ($n=5$). Except for differences in tissue regression, these results largely agree with the conclusion of Dubois (Dubois, 1949) that irradiated anterior tissue in partially irradiated animals regresses back towards the shielded tissue.

Next, we looked directly at the spatial distribution of SCs in partially irradiated animals by WISH for the SC marker *Smed-piwi-1* (Reddien et al., 2005b) (Fig. 1F). As predicted, we saw well-defined borders between the irradiated tissues, which were devoid of SCs, and the shielded tissue, which contained *piwi*(+) SCs (Fig. 1G, arrows). Over 9 days post-irradiation (dpi), no qualitative or quantitative changes in the size or shape of the SC-containing area were noted (Fig. 1G-K, $P>0.1$, one-way pairwise ANOVA). We conclude from these data that SCs do not undergo substantial migration into irradiated tissue in the absence of wounding within this timeframe.

Stem cell transplantation rescues lethally irradiated planaria

To study SC migration further, we developed an efficacious and reproducible method of tissue transplantation (Fig. 2A). When healthy tissue was successfully grafted into lethally irradiated planaria the hosts were always rescued ($n>100$) (Fig. 2B). This was in contrast to a recently reported cell transplantation technique, which impressively rescued lethally irradiated hosts with a single SC, but did so at low frequency ($n=7/130$) (Wagner et al., 2011). Long-term follow-up revealed that rescued planarians ($n>100$) show no difference in mortality from the common CIW4 strain. Conversely, transplantation of lethally irradiated grafts into lethally irradiated hosts (Fig. 2C) had no influence on survival, resulting in head regression, ventral curling and death. Furthermore, endpoint analysis of rescued animals (Fig. 2D) showed by WISH that the SC compartment is repopulated indistinguishably from that of wild-type worms (compare with Fig. 1F).

Conversion of asexual to sexual planaria through stem cell transplantation

To investigate the relative contribution to long-term tissue homeostasis of the host versus donor cells, we attempted to rescue lethally irradiated asexual planaria with healthy grafts from the genetically distinct sexual biotype. The asexual and sexual biotypes of *S. mediterranea* are characterized not only by differences in reproduction, pigmentation, maximal size and anatomy, but also by a large chromosomal translocation present only in asexual animals (Saló and Baguñà, 1985). At 7 days post-transplantation (dpt), the irradiated asexual host and sexual graft remained distinguishable (Fig. 2E, arrowhead) and the ventral surface of grafted animals showed no signs of sexual organs (Fig. 2E'). After two months of tissue turnover, however, rescued animals clearly displayed sexual pigmentation (Fig. 2E, 63 dpt) as well as a gonopore (Fig. 2E", arrow). Not only did these animals take on the sexual biotype physical characteristics but they also were functionally sexualized ($n=9$). Furthermore, karyotyping of these sexualized animals revealed only the sexual karyotype (supplementary material Fig. S3). Control non-irradiated asexuals that received sexual grafts did not sexualize during the length of the experiment ($n=9$), suggesting that sexualization is not due to some dominant factor but rather cell replacement. These data, combined with the high rate of planarian tissue turnover (Eisenhoffer et al., 2008), suggested that the sexual SCs eventually reconstituted all of the irradiated asexual host tissues. These findings support the conclusion of others that transplanted asexual SCs can convert irradiated sexual animals; however, these studies either lacked the functional outcome obvious in asexual to sexual conversion (Wagner et al., 2011) or did not show data for sexualization (Baguñà et al., 1989).

Transplanted stem cells repopulate host tissues but remain collectively totipotent

Rescue of lethally irradiated host tissue by healthy grafts suggested that SCs were repopulating the empty SC compartment within the host. To determine whether repopulation was taking place, we
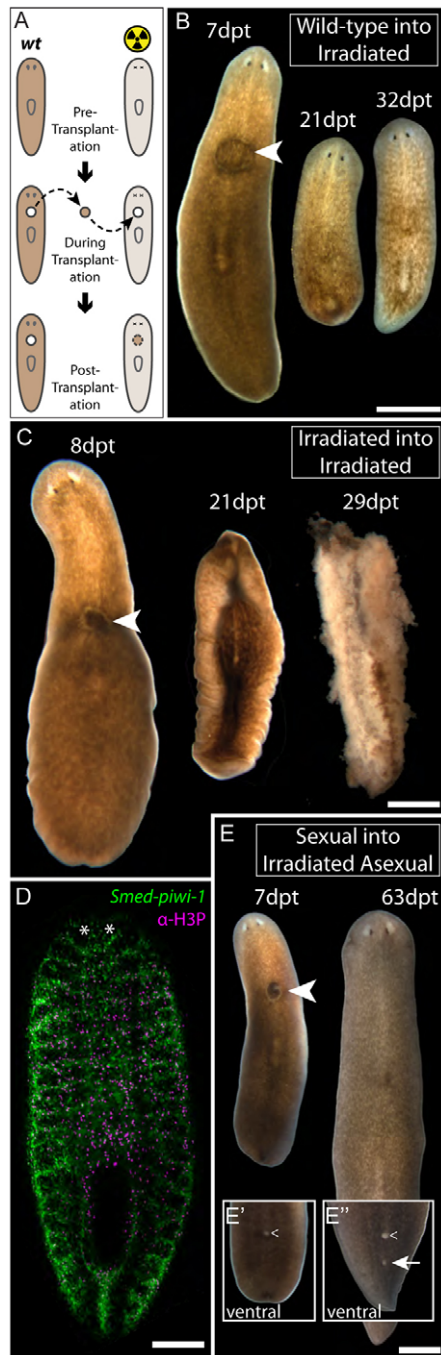
Fig. 2. Transplantation rescues tissue homeostasis in lethally irradiated hosts by SC repopulation. (**A**) Tissue from a wild-type donor was grafted into a lethally irradiated (100 Gy) recipient. (**B**) Live images of irradiated host grafted with wild-type tissue (arrowhead) at 7, 21 and 32 days dpt. (**C**) Irradiated donor grafted with irradiated tissue at 8, 21 and 29 dpt, displaying head regression, ventral curling (21 dpt, ventral view) and total lysis (29 dpt). (**D**) Labeling for all (*piwi*) and mitotic (anti-H3P) SCs in 32 dpt animal was indistinguishable from wild-type animals (Reddien et al., 2005b). Asterisks indicate photoreceptors. (**E-E″**) Live images of irradiated asexual biotype host grafted with wild-type sexual tissue at 7 and 63 dpt. Darker pigmentation of sexual graft (E, arrowhead) was evident at 7 dpt. (E′) At 7 dpt, grafted animals lacked gonopores. Chevron indicates pharyngeal opening. By 63 dpt, animals developed a gonopore (E″, arrow) and darker pigmentation. Beyond 63 dpt, animals regularly laid eggs. Scale bars: in B,C,E, 1 mm; in D, 500 μm.

looked at the position of all SCs by WISH in grafted animals (Fig. 3A-F). Concordantly, at 2 dpt we observed that irradiated hosts lacked *piwi*(+) SCs except for those contained within the graft and a small number that had migrated into host tissue (Fig. 3A). By 3 dpt, a considerable number of *piwi*(+) SCs had appeared within the host (Fig. 3B, arrowheads), and a progressive repopulation was observed over successive days (Fig. 3C-F). Altering transplantation location did not affect repopulation, nor did we detect any spontaneous *piwi* expression or new SC progeny in irradiated hosts grafted with irradiated tissue (supplementary material Fig. S4).

Congruent with the loss of *piwi* expression, lethally irradiated planaria are completely devoid of mitotic activity by 24 hours (Reddien et al., 2005a). Predictably, at 2 dpt, only a small number of mitoses were seen in the host (Fig. 3G) followed by progressively more at later time points (Fig. 3H-J), suggesting that the repopulating SCs were mitotically active. Quantification confirmed that SC repopulation progressed radially with a slight longitudinal bias (Fig. 3K).

We investigated next whether the migrating mitotically active *piwi*(+) SCs are functionally equivalent to those in the graft using serial transplantations. Following a primary transplantation (Fig. 2A), the newly grafted host was used as a donor, and tissue taken from a region anterior to the primary graft was transplanted into a naive irradiated planarian (Fig. 3L). The secondary graft, therefore, contained cells that had migrated into the irradiated primary host (Fig. 3M), thus resulting in the successful serial transplantation of SCs into the final host (Fig. 3N).

Scoring survival of serial transplantations revealed that grafts containing migrating SCs were capable of rescuing lethally irradiated hosts (Fig. 3O). However, different rates of survival were observed depending on the amount of time between the primary and secondary transplantations. For instance, no (*n*=0/10) animals survived when there were only 5 days between transplantations. However, when the time was increased to 10, 15 or 20 days, ~36% (*n*=4/11), ~77% (*n*=13/17) and 100% (*n*=12/12) of the final hosts survived, respectively. We concluded that increased time between transplantations resulted in more migrating SCs in the secondary graft and, therefore, a correlation with increased survival.

Transplanted stem cells restore normal lineage progression

Having observed SC repopulation, we investigated next whether SC progeny lineages are also restored. After irradiation, loss of early (at 2 dpi) and late (at 4 dpi) SC progeny follows loss of the SC population (at 1 dpi) (Eisenhoffer et al., 2008), and altering the SC-progeny relationship has lethal consequences in planaria (Pearson and Sánchez Alvarado, 2010). Re-establishment of the normal SC-progeny lineage is therefore crucial for rescue. Additionally, characterization of SC progeny repopulation would provide key reference points against which underlying SC migrations could be evaluated.

In intact planaria, along all body axes, the SCs reside proximal to the gut, early progeny inhabit a layer distal to the SCs, and late progeny exist in a layer distal to the early progeny (Eisenhoffer et al., 2008) (Fig. 4A). During tissue homeostasis, SC progeny progress from the SC compartment distally, turning off expression of SC markers and turning on corresponding progeny markers as they transition through each zone. We therefore looked at the expression domains following transplantation of two routinely used progeny markers, *Smed-prog-1* [for clarity, *Smed-NB.21.11e* (Eisenhoffer et al., 2008) is referred to as *Smed-prog-1*] and *Smed-agat-1*, known to identify early and late SC progeny, respectively
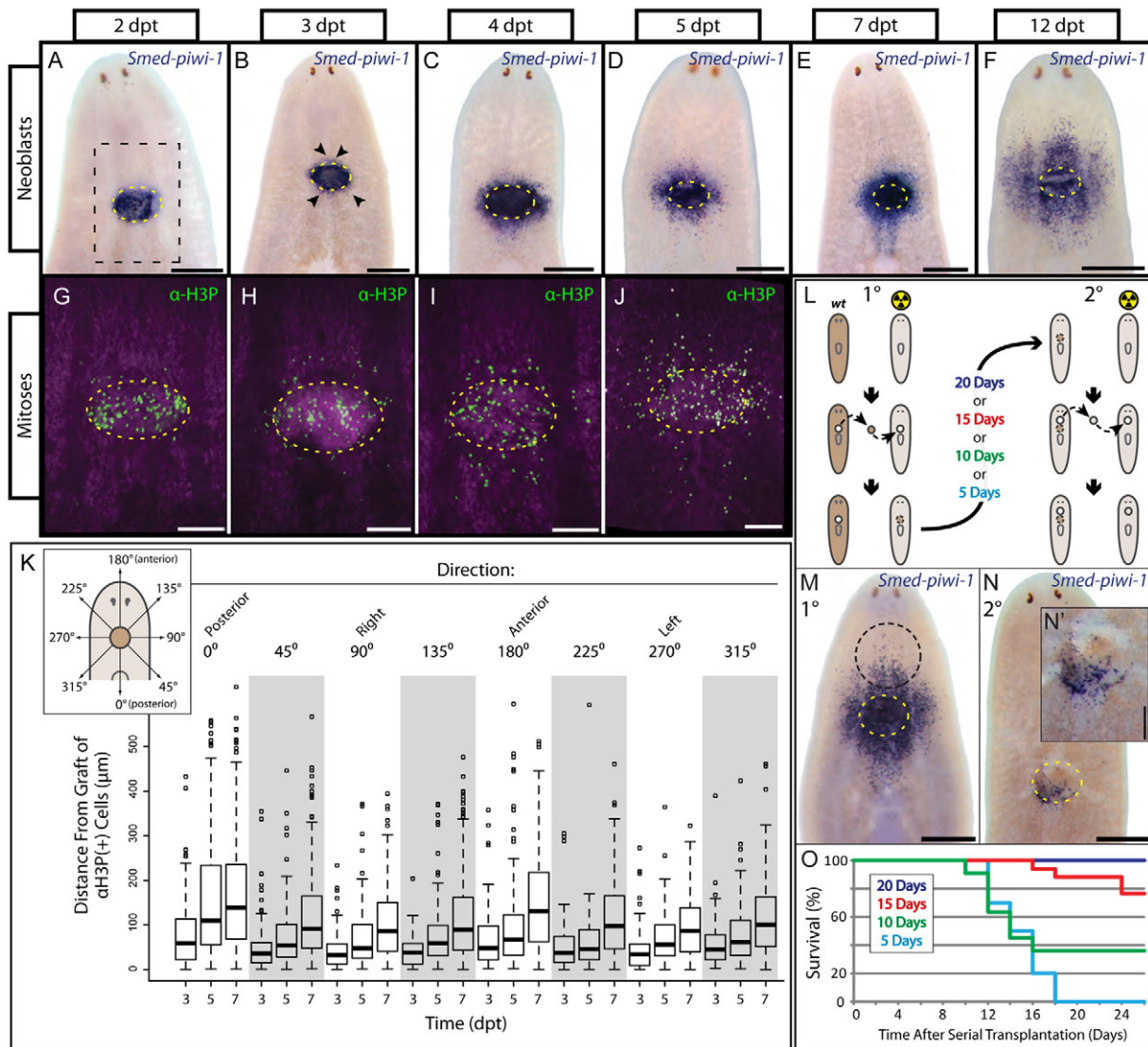
Fig. 3. Functionally multipotent, mitotically active SCs progressively repopulate lethally irradiated hosts. (A-F) SCs (*piwi*) in lethally irradiated hosts grafted with wild-type tissue at 2, 3, 4, 5, 7 and 12 dpt. Few SCs were observed outside the graft-host boundary at 2 dpt (A) but cells present in host tissue at 3 dpt (B, arrowheads) with progressively more by 4 (C), 5 (D) and 7 dpt (E). By 12 dpt (F), SCs spread to the lateral edges of the host. **(G-J)** Mitoses (anti-H3P) in graft region as indicated by the boxed area in A at 2, 3, 4 and 5 dpt. Lack of autofluorescence (G-J, magenta) revealed the graft-host boundary. Few H3P(+) cells were observed outside the graft at 2 dpt (G); however, more cells progressed further from the graft at 3 (H), 4 (I) and 5 (J) dpt. **(K)** Quantification in all directions (inset), showed uniform repopulation with a slight longitudinal bias (*n*=16, 11 and 17 at dpt 3, 5 and 7, respectively). Thick black lines represent median values, boxes represent interquartile ranges (IQRs) and whiskers represent ±1.5×IQR. **(L)** Serial transplantation scheme showing lengths of time allowed to pass between transplantations (5-20 days). **(M)** WISH for *piwi* 10 days following primary transplantation with the presumptive secondary graft tissue (dashed black circle) indicated. **(N)** Serially transplanted SCs labeled 3 days following secondary transplantation at single cell resolution. N' shows graft area magnified. **(O)** Serial transplantation survival curves for experiments in which 20 (blue, *n*=12), 15 (red, *n*=17), 10 (green, *n*=11) or 5 days (cyan, *n*=10) passed between primary and secondary transplantations. Yellow dashed circles and ellipses indicate graft area. Scale bars: in A-F,M-N, 500 μm; G-J,N', 200 μm.

(Fig. 4). Our earliest time point (4 dpt, 5 dpi) follows the depletion of host *prog* and *agat* (4 dpi) and therefore identified progeny that are derived from the graft (supplementary material Fig. S4).

We found that both early (Fig. 4B,D,H,J,N) and late (Fig. 4C,E,K,Q) progeny disperse from the graft analogous to repopulating mitotically active SCs (Fig. 3), complete with longitudinal bias. Similar to the positional relationship between early and late progeny in intact worms, the *prog* zone of expression appeared smaller than the *agat* zone of expression at 7 and 12 dpt

in most animals (Fig. 4B versus 4C, and 4D versus 4E). Staining for both *piwi* and *prog* in the same animal (Fig. 4F) revealed that the wild-type positional relationship between SCs and their early progeny may be re-established as early as 4 dpt.

Using SC and progeny positional relationships as readout for the status of the lineage, we sought to determine the earliest time point at which each positional relationship was re-established. WISH for *piwi* and *prog* showed that their relationship is re-established as early as 4 dpt (Fig. 4G-I). Whereas at 4 dpt *prog* and *agat* cells inhabit
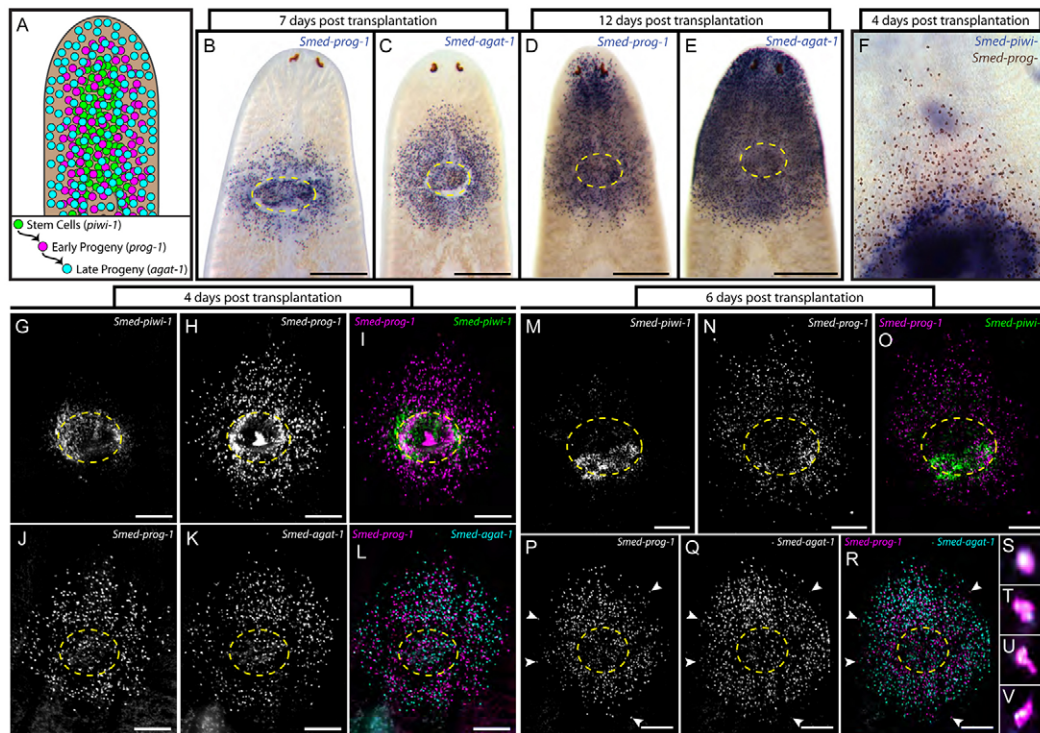
Fig. 4. Repopulation re-establishes normal SC-progeny positional relationships. (**A**) Nested positional relationships between SCs and progeny during tissue homeostasis. (**B,C**) WISH for early progeny (*Smed-prog-1*) at 7 dpt (B) showing smaller zone of expression than late progeny (*Smed-agat-1*) (C) in transplantation rescued animals. (**D,E**) Positional relationship between early (D) and late (E) progeny in anterior ends of 12 dpt animals. (**F**) Anterior graft area at 4 dpt showing early progeny (brown) distal to SCs (blue). (**G-I**) Double WISH showing the smaller SC domain (G) compared with early progeny domain (H) at 4 dpt. (**J-L**) WISH for early (J) and late (K) progeny at 4 dpt showing similar domains and lack of wild-type positional relationship. (**M-O**) Re-established relationship between SCs (M) and early progeny (N) is maintained. (**P,Q**) At 6 dpt, the early progeny zone (P) is smaller than the late progeny zone (Q). Arrowheads indicate co-expressing cells. (**R-V**) *Agat* late progeny cells are predominately distal to *prog* cells. Furthest distal *prog*-expressing cells (R, arrowheads) revealed low level co-expression of *agat* (S-V, single confocal slices). Yellow dashed ellipses indicate graft area. Scale bars: in B-E, 500 μm; in G-R, 200 μm.

similar zones (Fig. 4J-L), indicating that their positional relationship had yet to be restored. Not until 6 dpt was the relationship between late progeny and early progeny re-established (Fig. 4P-R). At 6 dpt, the re-established SC and early progeny relationship was maintained (Fig. 4M-O). Also, the presence of transitional cells (both *prog*- and *agat*-expressing) at the most distal extent of the early progeny zone (Fig. 4S-V) further indicated re-establishment of the lineage. We conclude that within a week of transplantation repopulating SCs re-establish characteristics of the normal SC lineage.

Amputation increases dispersion and induces directional recruitment of stem cells

Having described SC repopulation, we tested whether regeneration is restored in these animals. Regeneration was assayed by performing transplantations, decapitating (Fig. 5A) and then scoring for the appearance of blastemas and photoreceptors. Transplantation itself did not affect head regeneration (Fig. 5B,C). Interestingly, although irradiated hosts grafted with healthy tissue regenerated heads following amputation, regeneration was delayed (Fig. 5D,E). We attributed this delay to the time necessary for SCs in the graft to migrate through the irradiated tissue and reach the amputation plane. As expected, irradiated hosts grafted with irradiated tissue did not regenerate (Fig. 5F,G).

We investigated next whether the migration of repopulating SCs is altered by amputation. We compared SC migration in grafted animals that were either left intact or decapitated (Fig. 5A).

Qualitatively, SCs in 7 dpt decapitated animals increased their migration relative to their intact cohorts (Fig. 5H versus 5I) and SCs were seen as far anterior as the amputation plane (Fig. 5I, arrows), having migrated >500 μm in as few as 4 days post-amputation (dpa). A corresponding response to amputation was seen when mitotic SC location was evaluated (Fig. 5J,K).

We then measured the distance covered by SCs radiating out from the graft in both intact and decapitated animals (Fig. 5L). As predicted, the decapitated animals showed a highly significant increase ($P<0.002$) in the distance traveled by anteriorly directed SCs compared with non-decapitated animals (Fig. 5L). Surprisingly, increases ($0.01<P<0.02$) in SC migration following decapitation were also found in all other directions (Fig. 5L). However, in decapitated animals, the increase in anteriorly directed cells was significantly greater ($P<0.05$) than that of posteriorly directed cells. Quantification of mitotic SCs also revealed a significant increase following decapitation (Fig. 5M). These data suggest that decapitation during repopulation induced not only a global increase in SC dispersion, but also a specific increase in SC recruitment towards the amputation.

Although transplantation is highly effective for studying SC repopulation and function, recruitment analysis is complicated by the wound caused during transplantation (supplementary material Fig. S4) and the variability intrinsic in individual microsurgeries. Therefore, to determine whether SCs respond to amputation directionally as the transplantation evidence suggested, we
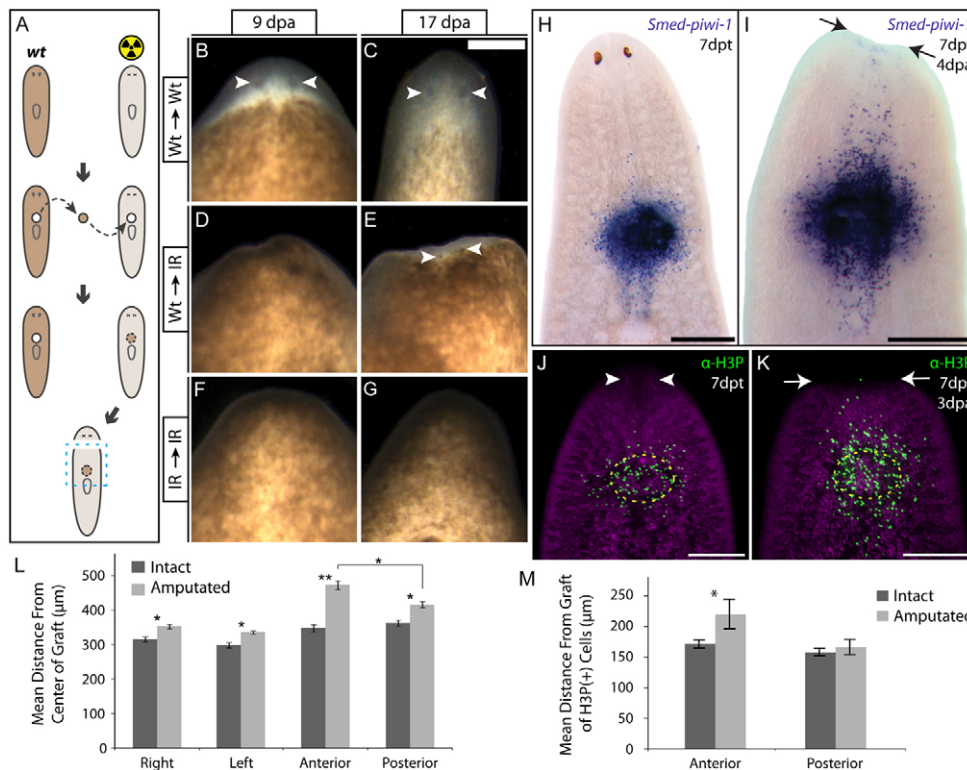
Fig. 5. Transplantation rescues regeneration and additional amputation increases SC migration. (**A**) Transplantations followed by decapitation 2-3 days after grafting. (**B,C**) Live images of decapitated, non-irradiated (Wt) host, control transplantation, showing anterior blastema at 9 dpa (B) and a reformed head at 17 dpa (C). (**D,E**) Delayed regeneration in decapitated lethally irradiated (IR) host grafted with non-irradiated tissue showed no blastema at 9 dpa (D) and small blastema at 17 dpa (E). Although delayed, these animals complete head regeneration. (**F,G**) Negative controls showed no regeneration. (**H,I**) Compared with non-decapitated animal (H, image from Fig. 3E for reference) migration of SCs in 7 dpt and 4 dpa animals (I) was increased and shifted anteriorly with SCs present at the amputation (arrows). (**J,K**) Staining for mitotic cells (anti-H3P) in non-decapitated (J) and decapitated (K) grafted animals. (**L**) Quantitative impact of amputation (I, $n=3$) on the position of SCs was compared with non-decapitated controls (H, $n=3$) at 7 dpt. The greatest increase ($P<0.002$) following amputation was seen in the anterior direction. Increases ($0.01<P<0.02$) following amputation were also seen in all other directions. (**M**) Quantification of mitotic cell positions in grafted animals also revealed a significant increase in anterior migration following amputation ($n=4$) compared with intact ($n=15$). Error bars are s.e.m. *$P<0.05$, **$P<0.005$ by Wilcoxon rank sum test. Photoreceptors are indicated by arrowheads. Scale bars: 500 µm.

performed partial irradiations and then amputated (Fig. 6A,B). Staining for *piwi* in decapitated partially irradiated animals clearly showed SCs in the anterior irradiated tissue at 5 dpa (Fig. 6B) in contrast to intact controls (Fig. 6A). The anterior (Fig. 6C) and posterior (Fig. 6C′) boundaries between the stem-cell-occupied shielded tissue and the stem-cell-devoid irradiated tissue in intact animals was clearly discernible at 3 dpi. Likewise, the boundaries (Fig. 6D,D′) of animals decapitated at 3 dpi and fixed immediately were also clear, indicating that amputation did not physically affect SC position. Although the SCs at the boundaries of 9 dpi intact planaria (Fig. 6E,E′) were slightly more dispersed than those at 3 dpi (Fig. 6C,C′), the most anterior and posterior regions remained largely devoid of SCs. Conversely, 9 dpi decapitated animals showed SCs at the anterior boundary and many SCs throughout the anterior region (Fig. 6F, arrowhead). Strikingly, the posterior boundaries of the very same decapitated animals remained defined (Fig. 6F′) and comparable to controls (Fig. 6E′). The apparent SC response at anterior but not posterior boundaries suggested that SCs might be directionally recruited by the anterior amputation.

These observations suggested that SC dispersion at anterior and posterior boundaries could be used to measure directional recruitment. We therefore quantified anterior boundary dispersion in partially irradiated animals that had been left intact or subjected

to anterior, posterior, or both amputations. We found that at 3 dpi, the day of amputation, there was no significant difference between intact and amputated animals (Fig. 6G,H). However, when animals were fixed at 2, 4 or 6 days following anterior amputation the anterior boundaries showed large increases in dispersion compared with controls (Fig. 6G, red versus blue). Interestingly, anterior boundaries of animals amputated posteriorly showed levels of dispersion equivalent to intact animals (Fig. 6G, 7 dpi green versus blue), indicating that, although SCs at the anterior boundary migrate anteriorly after decapitation, they do not migrate anteriorly after a posterior amputation. Furthermore, animals amputated both anteriorly and posteriorly showed dispersion at their anterior boundaries that was significantly greater than intact controls (Fig. 6G, yellow versus blue) but also significantly less than animals amputated only anteriorly (Fig. 6G, 7 dpi yellow versus red). This result might indicate competition for SCs by opposing wounds and further supports the existence of amputation-directed SC migration.

We next repeated our analysis of dispersion on posterior boundaries in the same animals and found largely congruent results. Predictably, SC dispersion at posterior boundaries was only significantly increased by posterior amputation (Fig. 6H, 7 dpi green versus blue or red), indicating that SCs migrate posteriorly in response to a posterior amputation but do not migrate posteriorly
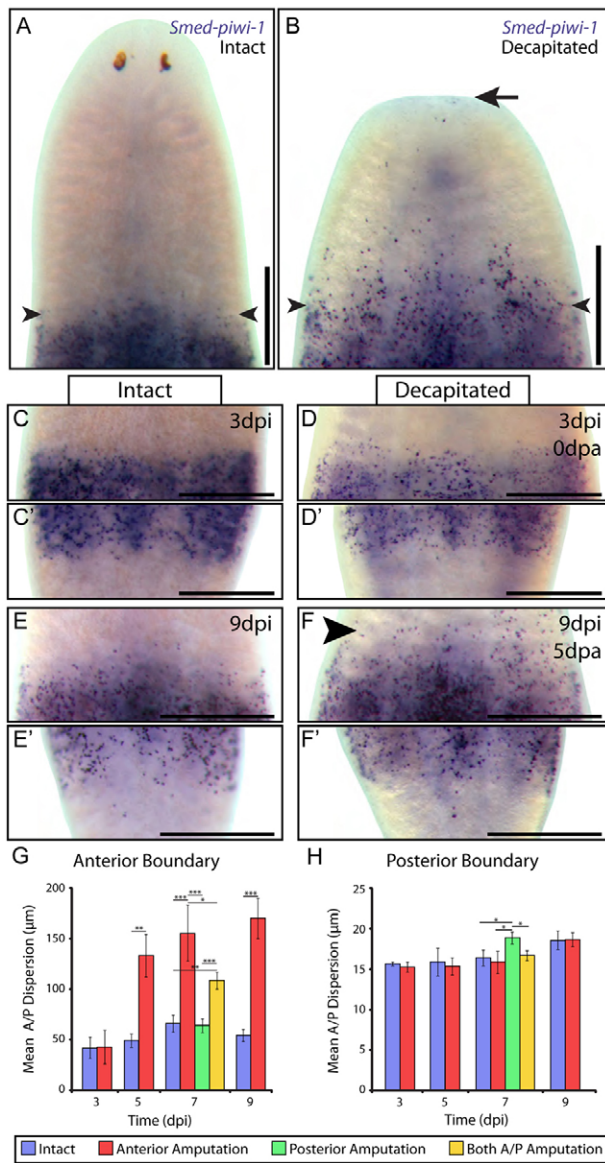
Fig. 6. Following amputation, SCs are recruited towards wounds. (**A**) Anterior of partially irradiated animals revealed a clean boundary (arrowheads) even at 9 dpi and a complete lack of SCs anteriorly. (**B**) Corresponding (9 dpi) decapitated (5 dpa) animals show SCs dispersed anterior to the estimated boundary (arrowheads) and at the amputation plane (arrow). (**C-F′**) The anterior (C) and posterior (C′) SC boundaries of intact partially irradiated animals at 3 dpi showed little dispersion. (D,D′) Boundaries of 3 dpi animals decapitated hours before fixation. Intact animal boundaries at 9 dpi (E,E′) showed slightly more dispersion compared with those at 3 dpi (C,C′). (F) SCs were dispersed and present far anterior of the boundary (arrowhead) in decapitated (5 dpa) 9 dpi animals. Posterior boundary (F′) showed levels of dispersion comparable to intact controls (E′). (**G,H**) Anterior/posterior (A/P) dispersion was quantified at anterior (G) and posterior (H) boundaries in intact, anteriorly, posteriorly, or both anteriorly and posteriorly amputated animals at 3, 5, 7 and 9 dpi, corresponding to 0, 2, 4 and 6 dpa, respectively. See text for analysis. Intact: n=3, 6, 11 and 8 for dpi 3, 5, 7 and 9, respectively. Anterior amputation: n=3, 8, 7 and 10 for dpi 3, 5, 7 and 9, respectively. Posterior amputation: n=12. Both A/P amputation: n=18. *P<0.05, **P<0.01,***P<0.001, one-sided Wilcoxon rank sum test. Error bars indicate s.e.m. Scale bars: 500 μm.

following decapitation. Additionally, we saw no significant difference at the posterior boundaries between intact controls and anteriorly amputated animals (Fig. 6H). Surprisingly, we did not see a significant increase at the posterior boundary in animals amputated both posteriorly and anteriorly (Fig. 6H, 7 dpi yellow versus blue). This could be due to a lack of sensitivity in the measurement because of the inherently lower levels of dispersion at posterior boundaries (compare y-axes in Fig. 6G and 6H), or it could reflect a biological difference between the ability of anterior and posterior wounds to recruit SCs. Altogether, our data support the conclusion that SCs are recruited, i.e. migrate in response to amputation in a directional manner.

Stem cells appear first at the amputation, migrating beyond their progeny
Seeking to determine what influence SC recruitment might have on progeny production, we evaluated SC and progeny positions after transplantation with decapitation (Fig. 7A,B). Strikingly, co-staining for *piwi* and *prog* revealed a dramatic shift, as SCs were now observed anterior to the early progeny (Fig. 7A) and at the amputation site (Fig. 7A, arrows, 7A′). Interestingly, SCs were dispersed between the graft and the amputation (Fig. 7A), suggesting that, although altered, the migration was continuous. In replicates in which the distance from the graft to the amputation plane was shorter, dense groups of late progeny were seen at the amputation (Fig. 7B, arrows) and SCs were present at least as anterior as the most anterior progeny (Fig. 7B′).

Our data indicate that SCs not only migrate beyond the early progeny but also serve as a new concentrated source of progeny once they reach the amputation. The data show that, for a given time point, animals with a longer distance between graft and amputation are significantly (P<0.0005, Kruskal-Wallis rank sum test) more likely to have only SCs present at the amputation plane (supplementary material Fig. S5). Thus, we conclude that the SCs were first to reach the wound and that progeny appeared second, either by migration or differentiation. These data combined with the known 4- to 5-day life-span of late progeny cells post irradiation (Eisenhoffer et al., 2008) indicated that some portion of the late progeny observed at the amputation site were derived de novo from migrating SCs either en route to or at the wound. Regardless, these results clearly demonstrated that the SC-progeny relationships, re-established during repopulation, are fundamentally altered by amputation, further supporting the existence of an active and highly dynamic mechanism for wound-activated SC recruitment in planaria.

DISCUSSION
Stem cell ablation is insufficient to trigger stem cell migration and repopulation
The maintenance of tissues subjected to physiological wear and tear generally depends on balancing cell proliferation and turnover. Although mechanisms are likely to exist to minimize SC turnover while maximizing their proliferative and differentiation capacity (Ohlstein and Spradling, 2007; Morrison and Spradling, 2008; Barker et al., 2010; Verheyen and Clevers, 2010), like all other cells, SCs eventually turn over (Molofsky et al., 2006; He et al., 2009). Does loss of SCs signal surviving cells to mobilize and occupy the vacated niches? In *Drosophila*, ablation of SCs in the testis or ovary results not in the repopulation of the niche by other SCs but rather by the de-differentiation of their progeny, which then occupy the vacated space (Brawley and Matunis, 2004; Kai and Spradling, 2004). By contrast, following elimination of HSCs,
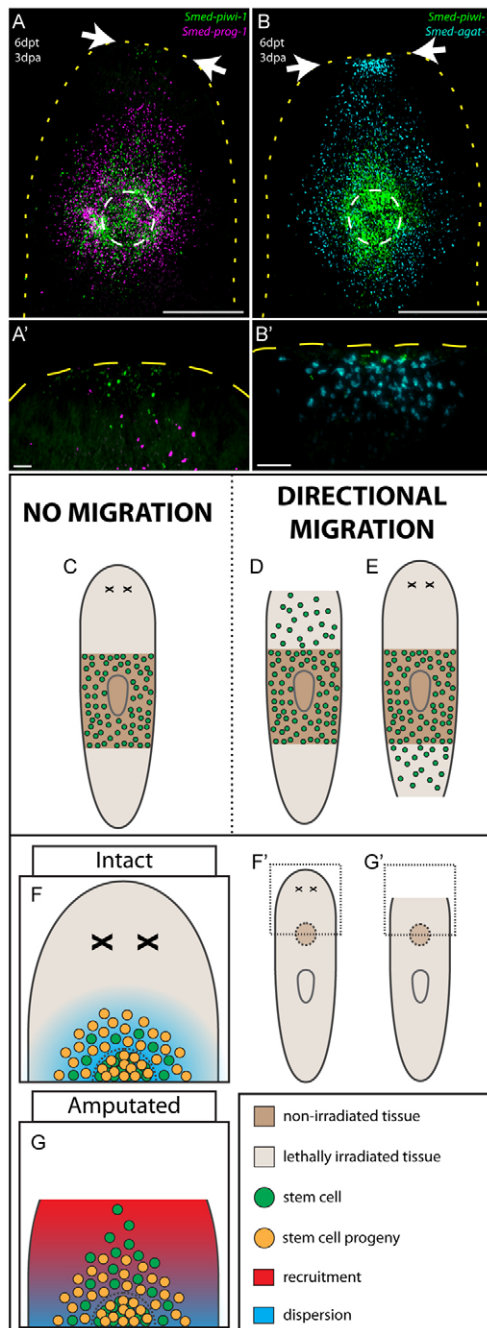
Fig. 7. Amputation-induced directional recruitment alters the relationship between SCs and their progeny. (A,A′) The positions of SCs (*piwi*) and early progeny (*prog*) after transplantation and decapitation at 6 dpt and 3 dpa (compare with Fig. 4O). SC population was continuous from graft (white dashed circle) to amputation plane (arrows in A and B). Magnification of amputation plane (A′) shows SCs (green) at wound site anterior to early progeny (magenta). **(B,B′)** SC and late progeny (*agat*) staining at 6 dpt and 3 dpa (compare with Fig. 4R). **(B′)** Magnified view shows SCs (green) slightly anterior to late progeny (cyan) and large group of late progeny just posterior to amputation site. Animals are outlined by dashed yellow line. Magnified projections (A′,B′) were obtained separately from overviews. Scale bars: in A,B, 500 μm; in A′,B′, 50 μm. **(C)** In the absence of wounding, SCs in partially irradiated animals are not induced to migrate. **(D)** Anterior amputation triggers wound signals that mobilize and recruit SCs. **(E)** Posterior amputation also triggers mobilization and recruitment. **(F,F′)** The wound from transplantation induces SC motility and the repopulating SCs produce progeny as they slowly invade host tissues (F′ shows the area illustrated). **(G,G′)** Anterior amputation recruits repopulating SCs, either accelerating SC anterior migration or inducing anteriorly migrating SCs to repress their progeny production such that SCs migrate beyond the progeny zone (G′ shows the area illustrated).

obvious clonal expansion of the SCs at the boundary between irradiated and shielded tissue, probably because our experiments were completed before clonal expansion would be apparent (Wagner et al., 2011).

Because of the highly proliferative nature of planarian SCs, it is difficult to determine the point at which a switch is made from normal homeostatic proliferation to clonal expansion during repopulation. Furthermore, whether some unidentified event is required to trigger clonal expansion is unknown. Likewise, the absence of both a mitotic response (Baguñà, 1976; Wenemoser and Reddien, 2010) and expression of known wound-induced molecules in irradiated planaria (Petersen and Reddien, 2009; Gurley et al., 2010), strongly suggest that irradiation alone does not induce a wound response. The lack of migration and wound signaling following partial irradiation is in contrast to increased apoptosis observed in irradiated tissue (Pellettieri et al., 2010). Therefore, although planaria display significant cellular responses to irradiation, emptying planarian tissues of SCs is clearly insufficient to induce SC migration and repopulation.

Loss of tissue integrity is required to trigger stem cell mobilization
The necessity of a breech in tissue integrity to initiate a wound response is consistent not only with our partial irradiation data but also the data of Dubois (Dubois, 1949). Only after partially irradiated animals were amputated were SCs recruited (Fig. 7D,E). Likewise, only after irradiated tissues began to disintegrate, which may be akin to wounding, were regeneration (Fig. 1D,E) and SC migration (supplementary material Fig. S6) observed. A loss of tissue integrity preceding repopulation has been seen by others (Wagner et al., 2011), though the SC dynamics were not directly evaluated.

Clonogenic stem cells are contained within the migratory stem cell population
Clonogenic SCs in planaria are pluripotent and singly capable of rescuing irradiated hosts at low frequency (*n*=7/130) (Wagner et al., 2011). By contrast, all successful transplantations presented here

niche repopulation takes place only after SCs are reintroduced by transplantation (Zhong et al., 2002). Furthermore, ablation of endogenous SCs is not necessarily required for recolonization of the niche by introduced SCs as shown in clonal ascidians (Stoner et al., 1999; Laird et al., 2005; Voskoboynik et al., 2008). Whether or not these different modes of repopulation are taxa specific or reflect broader, fundamental traits of metazoan SC homeostasis remains unknown.

We sought to address this issue by selectively eliminating planarian SCs via partial irradiation (Fig. 1). Our data demonstrate that SC ablation alone does not induce SC mobilization in planaria (Fig. 7C). Our conclusion is supported by studies in which SCs were observed to remain in close proximity for weeks during clonal expansion (Wagner et al., 2011). Interestingly, we did not observe

resulted in long-term survival, demonstrating that clonogenic SCs, or cells capable of producing them, were always within the graft. Furthermore, the rescue of lethally irradiated animals by serial transplantation (Fig. 3O) suggests that either clonogenic SCs are migratory or they are produced by migratory SCs. We estimate that ~168 migrating SCs were necessary for rescue (supplementary materials Fig. S7). This high number could be an indication that clonogenic SCs are rare within the migrating population or could be the result of our stringent survival assay. Nonetheless, the rescue of 100% of animals serially grafted 20 days following primary transplantation (Fig. 3O) strongly argues that clonogenic SCs repopulate the irradiated host tissue, retain pluripotency and remain capable of expanding and rescuing subsequent hosts.

Wounding mobilizes stem cells out of their niche, allowing niche repopulation

SC ablation alone did not trigger migration (Fig. 1G,K). Although we cannot rule out a change in SC density within the shielded compartment, if such an increase occurred it did not result in spreading of SCs into the irradiated regions. Only after wounding did SCs mobilize out of shielded niches and into irradiated tissues (Fig. 7D,E). Similarly, following transplantation, SCs migrated out of the tissue graft probably owing to the presence of the wound incurred during the transplantation itself (Fig. 7F). Following repopulation, animals from both contexts were indistinguishable from wild type, indicating that the irradiated tissues are competent to support SCs. Mobilized SCs, therefore, either re-enter stable empty niches or rebuild niches within the irradiated tissue.

Once mobilized, SCs occupy irradiated or physically damaged tissue, such that these tissues are stabilized and homeostasis is restored. This is in contrast to partially irradiated animals that were not wounded and therefore lacked the SC mobilization necessary to repopulate, repair and maintain the damaged tissue, resulting in tissue regression. Thus, our results define a powerful experimental paradigm for dissecting the in vivo mechanisms controlling initiation and termination of SC movements within tissues.

Stem cells home to amputation sites

The complex interplay between wounding frequency, number of wounds, wound geometry and the cells affecting a response has been largely ignored in previous work. As such, conflicting conclusions exist regarding whether or not planarian SCs migrate (Flickinger, 1964; Saló and Baguñà, 1985). Our results, particularly the quantitative measurements, indicate that SCs actively home to amputation sites. For example, SCs in partially irradiated doubly amputated animals home less effectively than do SCs in singly amputated animals, presumably owing to competing wound signals. Likewise, the SCs already mobilized following transplantation respond to an additional amputation by deviating to home directly to the amputation site (Fig. 7G). Remarkably, this anterior recruitment is accompanied by either accelerated migration or repressed differentiation in SCs migrating anteriorly such that SCs were capable of outrunning their progeny (Fig. 7F versus 7G). Our finding that SCs appear to be capable of integrating multiple wound signals might partially explain the ability of planarians to regenerate from, not only a myriad of different single wounds, but also many combinations of multiple wounds.

Conclusion

We found that the physical perturbation of tissues triggers the directional mobilization of SCs to sites of injury and that partial elimination of SCs by irradiation is insufficient to trigger

recruitment. These findings strongly suggest that migration factors capable of directing SC migration are activated upon amputation. Although the existence of planarian wound signals has long been postulated, evidence for their existence is sparse at best. Taken together, the presented results and novel assays, not only provide strong evidence for the actuality of such factors, but also provide a novel experimental paradigm with which to discover wound signal factors and define their mechanisms of action.

Competing interests statement
The authors declare no competing financial interests.

Supplementary material
Supplementary material available online at
http://dev.biologists.org/lookup/suppl/doi:10.1242/dev.082099/-/DC1

References
Baguñà, J. (1976). Mitosis in the intact and regenerating planarian Dugesia mediterranea n.sp. II. Mitotic studies during regeneration, and a possible mechanism of blastema formation. *J. Exp. Zool.* **195**, 65-79.
Baguñà, J., Saló, E. and Auladell, C. (1989). Regeneration and pattern formation in planarians. III. Evidence that neoblasts are totipotent stem cells and the source of blastema cells. *Development* **107**, 77-86.
Bardeen, C. and Baetjer, F. (1904). The inhibitive action of the Roentgen rays on regeneration in planarians. *J. Exp. Zool.* **1**, 191-195.
Barker, N., Bartfeld, S. and Clevers, H. (2010). Tissue-resident adult stem cell populations of rapidly self-renewing organs. *Cell Stem Cell* **7**, 656-670.
Blanpain, C., Lowry, W. E., Geoghegan, A., Polak, L. and Fuchs, E. (2004). Self-renewal, multipotency, and the existence of two cell populations within an epithelial stem cell niche. *Cell* **118**, 635-648.
Brawley, C. and Matunis, E. (2004). Regeneration of male germline stem cells by spermatogonial dedifferentiation in vivo. *Science* **304**, 1331-1334.
Cebrià, F. and Newmark, P. A. (2005). Planarian homologs of netrin and netrin receptor are required for proper regeneration of the central nervous system and the maintenance of nervous system architecture. *Development* **132**, 3691-3703.
Congdon, C. C. (1971). Bone marrow transplantation. *Science* **171**, 1116-1124.
Daley, G. Q. and Scadden, D. T. (2008). Prospects for stem cell-based therapy. *Cell* **132**, 544-548.
Dubois, F. (1949). Contribution á l 'ètude de la migration des cellules de règènèration chez les Planaires dulcicoles. *Bull. Biol. Fr. Belg.* **83**, 213-283.
Eisenhoffer, G. T., Kang, H. and Sánchez Alvarado, A. (2008). Molecular analysis of stem cells and their descendants during cell turnover and regeneration in the planarian Schmidtea mediterranea. *Cell Stem Cell* **3**, 327-339.
Fedecka-Bruner, B. (1965). *Regeneration in Animals and Related Problems* (ed. V. Kiortsis and H. A. L. Trampusch), pp. 185-192. Amsterdam, The Netherlands: North-Holland Publishing Company.
Flickinger, R. (1964). Isotopic evidence for a local origin of blastema cells in regenerating planarians. *Exp. Cell Res.* **34**, 403-406.
Gurley, K. A., Elliott, S. A., Simakov, O., Schmidt, H. A., Holstein, T. W. and Sánchez Alvarado, A. (2010). Expression of secreted Wnt pathway components reveals unexpected complexity of the planarian amputation response. *Dev. Biol.* **347**, 24-39.
Hayashi, T., Asami, M., Higuchi, S., Shibata, N. and Agata, K. (2006). Isolation of planarian X-ray-sensitive stem cells by fluorescence-activated cell sorting. *Dev. Growth Differ.* **48**, 371-380.
He, S., Iwashita, T., Buchstaller, J., Molofsky, A. V., Thomas, D. and Morrison, S. J. (2009). Bmi-1 over-expression in neural stem/progenitor cells increases proliferation and neurogenesis in culture but has little effect on these functions in vivo. *Dev. Biol.* **328**, 257-272.
Kai, T. and Spradling, A. (2004). Differentiating germ cells can revert into functional stem cells in Drosophila melanogaster ovaries. *Nature* **428**, 564-569.

Karp, J. M. and Leng Teo, G. S. (2009). Mesenchymal stem cell homing: the devil is in the details. *Cell Stem Cell* **4**, 206-216.

Kato, K., Orii, H., Watanabe, K. and Agata, K. (1999). The role of dorsoventral interaction in the onset of planarian regeneration. *Development* **126**, 1031-1040.

Kim, D., Hong, K. S. and Song, J. (2007). The present status of cell tracking methods in animal models using magnetic resonance imaging technology. *Mol. Cells* **23**, 132-137.

Laird, D. J., De Tomaso, A. W. and Weissman, I. L. (2005). Stem cells are units of natural selection in a colonial ascidian. *Cell* **123**, 1351-1360.

Laird, D. J., von Andrian, U. H. and Wagers, A. J. (2008). Stem cell trafficking in tissue development, growth, and disease. *Cell* **132**, 612-630.

Lehnert, G. (1891). Beobachtung an Landplanarien. *Arch. Naturgech.* **1**, 306-350.

Miller, W. and Kennedy, R. J. (1955). X-ray attenuation in lead, aluminum, and concrete in the range 275 to 525 kilovolts. *Radiology* **65**, 920-925.

Molofsky, A. V., Slutsky, S. G., Joseph, N. M., He, S., Pardal, R., Krishnamurthy, J., Sharpless, N. E. and Morrison, S. J. (2006). Increasing p16INK4a expression decreases forebrain progenitors and neurogenesis during ageing. *Nature* **443**, 448-452.

Morrison, S. J. and Spradling, A. C. (2008). Stem cells and niches: mechanisms that promote stem cell maintenance throughout life. *Cell* **132**, 598-611.

Newmark, P. A. and Sánchez Alvarado, A. (2000). Bromodeoxyuridine specifically labels the regenerative stem cells of planarians. *Dev. Biol.* **220**, 142-153.

Newmark, P. A. and Sánchez Alvarado, A. (2002). Not your father's planarian: a classic model enters the era of functional genomics. *Nat. Rev. Genet.* **3**, 210-219.

Ohlstein, B. and Spradling, A. (2007). Multipotent Drosophila intestinal stem cells specify daughter cell fates by differential notch signaling. *Science* **315**, 988-992.

Pearson, B. J. and Sánchez Alvarado, A. (2010). A planarian p53 homolog regulates proliferation and self-renewal in adult stem cell lineages. *Development* **137**, 213-221.

Pearson, B. J., Eisenhoffer, G. T., Gurley, K. A., Rink, J. C., Miller, D. E. and Sánchez Alvarado, A. (2009). Formaldehyde-based whole-mount in situ hybridization method for planarians. *Dev. Dyn.* **238**, 443-450.

Pellettieri, J., Fitzgerald, P., Watanabe, S., Mancuso, J., Green, D. R. and Sánchez Alvarado, A. (2010). Cell death and tissue remodeling in planarian regeneration. *Dev. Biol.* **338**, 76-85.

Petersen, C. P. and Reddien, P. W. (2009). A wound-induced Wnt expression program controls planarian regeneration polarity. *Proc. Natl. Acad. Sci. USA* **106**, 17061-17066.

Pittenger, M. F., Mackay, A. M., Beck, S. C., Jaiswal, R. K., Douglas, R., Mosca, J. D., Moorman, M. A., Simonetti, D. W., Craig, S. and Marshak, D. R. (1999). Multilineage potential of adult human mesenchymal stem cells. *Science* **284**, 143-147.

Reddien, P. W., Bermange, A. L., Murfitt, K. J., Jennings, J. R. and Sánchez Alvarado, A. (2005a). Identification of genes needed for regeneration, stem cell function, and tissue homeostasis by systematic gene perturbation in planaria. *Dev. Cell* **8**, 635-649.

Reddien, P. W., Oviedo, N. J., Jennings, J. R., Jenkin, J. C. and Sánchez Alvarado, A. (2005b). SMEDWI-2 is a PIWI-like protein that regulates planarian stem cells. *Science* **310**, 1327-1330.

Reya, T., Morrison, S. J., Clarke, M. F. and Weissman, I. L. (2001). Stem cells, cancer, and cancer stem cells. *Nature* **414**, 105-111.

Rietze, R. L., Valcanis, H., Brooker, G. F., Thomas, T., Voss, A. K. and Bartlett, P. F. (2001). Purification of a pluripotent neural stem cell from the adult mouse brain. *Nature* **412**, 736-739.

Saló, E. and Baguñà, J. (1985). Cell movement in intact and regenerating planarians. Quantitation using chromosomal, nuclear and cytoplasmic markers. *J. Embryol. Exp. Morphol.* **89**, 57-70.

Salo, E. and Baguna, J. (1986). Stimulation of cellular proliferation and differentiation in the intact and regenerating planarian Dugesia(G) tigrina by the neuropeptide substance P. *J. Exp. Zool.* **237**, 129-135.

Sánchez Alvarado, A., Newmark, P. A., Robb, S. M. and Juste, R. (2002). The Schmidtea mediterranea database as a molecular resource for studying platyhelminthes, stem cells and regeneration. *Development* **129**, 5659-5665.

Santos, F. (1929). Studies on transplantation in planaria. *Biological Bulletin* **57**, 188-197.

Sherwood, R. I., Christensen, J. L., Conboy, I. M., Conboy, M. J., Rando, T. A., Weissman, I. L. and Wagers, A. J. (2004). Isolation of adult mouse myogenic progenitors: functional heterogeneity of cells within and engrafting skeletal muscle. *Cell* **119**, 543-554.

Steele, V. and Lange, C. (1976). Effects of irradiation on stem cell response to differentiation inhibitors in the planarian Dugesia etrusca. *Radiat. Res.* **67**, 21-29.

Stéphan-Dubois, F. and Lender, T. (1956). Corrélations humorales dans la régénération de planaires paludicoles. *Ann. des Sc. Nat. Zool.* **18**, 223-230.

Stoner, D. S., Rinkevich, B. and Weissman, I. L. (1999). Heritable germ and somatic cell lineage competitions in chimeric colonial protochordates. *Proc. Natl. Acad. Sci. USA* **96**, 9148-9153.

Verheyen, E. M. and Clevers, H. (2010). Wnts as self-renewal factors: mammary stem cells and beyond. *Cell Stem Cell* **6**, 494-495.

Voskoboynik, A., Soen, Y., Rinkevich, Y., Rosner, A., Ueno, H., Reshef, R., Ishizuka, K. J., Palmeri, K. J., Moiseeva, E., Rinkevich, B. et al. (2008). Identification of the endostyle as a stem cell niche in a colonial chordate. *Cell Stem Cell* **3**, 456-464.

Wagner, D. E., Wang, I. E. and Reddien, P. W. (2011). Clonogenic neoblasts are pluripotent adult stem cells that underlie planarian regeneration. *Science* **332**, 811-816.

Wenemoser, D. and Reddien, P. W. (2010). Planarian regeneration involves distinct stem cell responses to wounds and tissue absence. *Dev. Biol.* **344**, 979-991.

Wolff, E. and Dubois, F. (1948). Sur la migration des cellules de régénération chez les planaires. *Rev. Suisse Zool.* **55**, 218-227.

Zhong, J. F., Zhan, Y., Anderson, W. F. and Zhao, Y. (2002). Murine hematopoietic stem cell distribution and proliferation in ablated and nonablated bone marrow transplantation. *Blood* **100**, 3521-3526.